

32-CRYSTAL POSITRON TRANSVERSE SECTION DETECTOR\*

J. S. Robertson, R. B. Marr, M. Rosenblum,

V. Radeka and Y. L. Yamamoto\*\*

Medical Research Center  
BROOKHAVEN NATIONAL LABORATORY  
Upton, L.I., New York  
11973

- \* Research supported by the U.S. Atomic Energy Commission
- \*\* Montreal Neurological Institute, McGill University,  
Montreal, Canada.

**NOTICE**

This report was prepared as an account of work sponsored by the United States Government. Neither the United States nor the United States Atomic Energy Commission, nor any of their employees, nor any of their contractors, subcontractors, or their employees, makes any warranty, express or implied, or assumes any legal liability or responsibility for the accuracy, completeness or usefulness of any information, apparatus, product or process disclosed, or represents that its use would not infringe privately owned rights.

**MASTER**

## 32-CRYSTAL POSITRON TRANSVERSE SECTION DETECTOR

J.S. Robertson, R. B. Marr, M. Rosenblum,

V. Radeka and YL.Yamamoto

### INTRODUCTION:

The medical use of the positron coincidence method began over 20 years ago with the application to the problem of locating brain tumors by Wrenn, Good and Handler (1). The basic principles of this method were more thoroughly described by Brownell and Sweet (2). The latter authors have subsequently led in the development of the method, and a report on the current status of the MGH positron camera is being presented by Brownell in the next paper at this symposium (3). The system to be discussed in this paper is a section scanner that uses thirty-two 3.2 cm (1½ inch) diameter NaI(Tl) crystals mounted in a 40 cm (15-¾ inch) diameter ring with the appropriate electronics for having every possible crystal pairing in a coincidence detection circuit. Figure 1 illustrates the geometry of the system. Activity at the darkened spot gives coincidence counts in the detector pairs connected by the lines shown, whereas other pairs do not register coincidence counts.

Figure 2 shows that some pairs are connected by lines that fall outside of the volume of interest, and these are ignored.

Figure 3 is a photograph of the apparatus showing one method of positioning the subject.

This method offers the advantage of a higher quantum utilization than can be achieved with fixed pairings (i.e. with each crystal in a

**MASTER**

coincidence circuit with only the crystal directly opposite it). The multicoincidence method also provides a type of data that may be used in a mathematical reconstruction, or mapping, of the distribution of activity in the slab seen by the detector system. In its present form the system does not give as good spatial resolution as do others described at this symposium, but there is a potential for improvement, such as using a larger number of small detectors.

The section scanning method differs from tomography in that blurring out of sources above and below the slab of interest is not involved.

#### THE DETECTOR SYSTEM

The original system has been described by Rankowitz et al (4). In the configuration indicated above, each crystal subtends a solid angle of about 0.16% of  $4\pi$  for a source in the center. By experiment it was found that for  $^{22}\text{Na}$  0.511  $\gamma$  rays, the singles counting rate per crystal is about 1670 cpm/ $\mu\text{Ci}$ , or 0.075% of the total  $\gamma$  ray pair production rate. The coincidence detection rate is about 0.02% of the total  $\gamma$  ray pair production rate per crystal pair or 0.64% for the 32 crystal array.

In addition to the ring of 32 crystals the original system included coincidence circuitry and a magnetic drum for data storage. Recent changes in the circuitry and in the data storage method have greatly improved the reliability and usefulness of the instrument.

In particular, the following changes have been made. Window amplifiers that enable suppression of gamma rays that do not fall into the spectrum peak corresponding to 0.511 MeV gamma rays have been added. The time resolution has been narrowed to 40-100 nanoseconds (adjustable) and the dead time for false inputs has been reduced to about 1  $\mu\text{sec}$ . Instead of storing the data on the magnetic drum, the system has been connected by cables to an XDS Sigma 2 digital computer and the data are stored in the core memory of the computer.

The coincidence circuitry now operates as follows. Following a triggering input signal, all input signals occurring in the next 40-100 nanoseconds are stored in a register and examined. The signals are rejected if there is an odd (1, 3, 5,.. etc.) number of detector inputs or if they are from two adjacent crystals. If these tests are passed, the contents of the first storage register are transferred to a second one, leaving the first one free to accept new inputs.

Within about  $3.5\mu$  sec the contents of the second register is examined and the circuit produces a 9-bit number identifying the crystal pair involved and which serves as a relative address for storage of the event in the computer memory. If the smaller angle having its vertex in the center of the ring and its arms on the two crystals is measured clockwise, the first 5 bits indicate number of the reference crystal (0 to 31) and the last 4 bits indicate the radial separation in units of crystal diameters (2 to 16). In this operation the circuit checks that there are exactly two detectors involved and that the radial separation between them is above a minimum selected to define the volume of interest. This minimum is subtracted from the actual separation number and only positive resultants are transmitted. If these tests are passed the 9 bit number produced and a flag bit (which is always = 1) are transferred to a first- in first- out 4 word buffer for transmission to the computer memory. The flag bit is used to indicate the presence of data. In the computer the data for each section is stored in core memory as a  $32 \times 16$  array. Up to 8 such arrays are stored at one time. For longer sequences the data are transferred to magnetic tape for recall at the time of analysis.

### DATA PROCESSING

As has been mentioned, the data obtained by the counting method described have a potential capability of describing the distribution of radioactivity in the slab defined by the intersection of the planes of the ring of crystals with the volume of interest. Extracting this information from the data, however, has posed a computing problem that until very recently had not been satisfactorily solved. Figure 4 illustrates the general problem, which is to reconstruct the original distribution of activity from the coincidence counting data.

In one of the early attempts at a solution (5) a linear transformation using matrix algebra was used. This was based on the concept that the counts,  $c_p$ , registered in a given detector pair,  $p$ , is the sum of the activities,  $r_s$ , in the volume elements,  $s$ , along the line (or cylinder) connecting the two crystals weighted by a detection efficiency, or geometry, factor,  $g_{ps}$  for each point. Thus the counts for a given pair are

$$c_p = \sum_{s=1}^{s=n} g_{ps} r_s \quad (1)$$

when  $n$  is the number of elements of volume in the column of interest. As a preliminary step in the data processing, the  $c_p$ 's are corrected for detector sensitivity and for their separation distance. The values for  $g_{ps}$  are obtained by measurement of point sources. The count vector,  $C$  is related to the activity rate vector,  $R$ , and the geometry matrix,  $G$ , through the equation

$$C = G \cdot R \quad (2)$$

In principle the solution of this is given by multiplying both sides of equation 2 by the inverse matrix,  $G^{-1}$ , giving

$$R = G^{-1} C \quad (3)$$

In practice, however, the matrix inversion method introduced very large errors when real data was processed, and techniques for avoiding this were sought.

The next stage of analysis (6) was based on the observation that the set of detector pairs that <sup>are</sup> separated by a given number,  $j$ , are insensitive to all radioactivity within a circle defined by the radius of the chord connecting a given pair as indicated in Figure 5. Thus the outer rings may be solved first, and this information used in simplifying the solution of succeeding inner rings. This "onion peel" method seemed useable, but errors introduced in the early steps pervaded the rest of the solution and often led to questionable results.

A more sophisticated approach was developed by Pincus (7). In this, the viewpoint was adopted that the observed counts  $C(i, j)$  for a given counter pair are a sampling of a continuous count function  $C(p, \theta)$ , where  $p$  indicates the distance from the center and  $\theta$  indicates the angular location of the chord  $(i, j)$ . The analysis used a Fourier series in an interpolation procedure to construct the required continuous function. Although this was an improvement over all prior methods tried, in practice this method introduced serious artifacts into the solution and further improvements were sought.

The method currently in use is based on a procedure described in detail by Marr (8). This procedure begins with the same concept of the count distribution function as above, but uses a different system of function transformations. In brief, it is shown that the points on the sampling mesh correspond to the zeroes of one of the classical Chebyshev polynomials of the second kind, and these polynomials are transforms of a system of orthogonal polynomials that describe the counting distribution. Thus a polynomial function in  $x$  and  $y$  can be reconstructed that yields a least squares fit of the data and that describes the distribution of radioactivity in the volume of interest. This procedure is computationally efficient and is the basis for the computer program currently in use.

The complete procedure can be described succinctly as follows:

Let  $N$  be the number of counters (= 32 in our case), with  $C(i_1, i_2)$  the (corrected) coincidence count data for the  $(i_1, i_2)$  counter pair. Assume that the counters are numbered in consecutive counter clockwise order, and choose Cartesian coordinates,  $x$  and  $y$ , so that  $x^2 + y^2 = 1$  is the equation for the circle defined by the counter array, with counter No. 1 lying on the positive  $x$ -axis.

For each pair of non-negative integers,  $n$  and  $k$ , satisfying  $n + 2k \leq N-2$ , compute coefficients  $\alpha_{n,k}$  and  $\beta_{n,k}$  according to the formula,

$$\begin{pmatrix} \alpha_{n,k} \\ \beta_{n,k} \end{pmatrix} = \frac{2 \sum_n (n+2k+1)}{N^2} \sum_{1 \leq i_1 < i_2 \leq N} \begin{pmatrix} \sin \\ \cos \end{pmatrix} \left[ (n+2k+1) (i_2 - i_1) \frac{\pi}{N} \right] \cdot C(i_1, i_2),$$

where  $\xi_0 = 1$  and  $\xi_n = 2$  for  $n > 1$ . (Note that  $\alpha_{0,k} = 0$  for all  $k$ ).

Then, as shown in (8), the polynomial least squares fit to the data of total degree  $M$  in  $x$  and  $y$  is given by

$$P^{(M)}(x,y) = \sum_{n=0}^M \sum_{k=0}^{\lfloor \frac{M-n}{2} \rfloor} [\alpha_{n,k} \sin n\psi + \beta_{n,k} \cos n\psi] r^n Q_{n,k}(r^2),$$

for any  $M \leq N - 2$ , where  $r$  and  $\psi$  are the usual polar coordinates of a point  $(x, y)$  and where, for each  $n$ ,  $\{Q_{n,k}(t) : k = 0, 1, 2 \dots\}$  is a system of (univariate) orthogonal polynomials for the weight function,  $t^n$ , on the interval  $(0, 1)$ , standardized so that  $Q_{n,k}(1) = 1$ , all  $n, k$ .

Computationally,  $P^{(M)}$  can be efficiently calculated at any point  $(x,y)$  by making use of rather simple linear recursion formulas, both for the array  $\{Q_{n,k}(t)\}$  and for the polynomials,  $S_n(x,y) = r^n \sin n\psi$  and  $C_n(x,y) = r^n \cos n\psi$ . Also, it may be noted that in the computation of  $\alpha_{n,k}$  and  $\beta_{n,k}$ , values of the sine and cosine functions are needed only at  $2N (= 64)$  distinct angles. These values can be easily retained to high precision in tabular form within the program. Hence, at no point in the reconstruction is it necessary to call upon trigonometric or other special function subroutines, and the entire procedure takes very little time (less than 3 seconds of CDC 6600 time to obtain the values of  $P^{(M)}$  on a  $40 \times 40$  grid of points).

#### DISPLAY

The computer program mentioned above produces an array of numbers that indicate the amounts of radioactivity at lattice points on a rectangular grid within the area of interest. This array can be printed out as a table



of numbers, or the numbers can be represented by shades of intensity, using a "grey wedge" of 32 shades obtained by overprinting selected printing characters.

Examples of the number array method for displaying the results obtained using simulated sources follow. Figure 6 shows the output for a 2 cm diameter source located in the boxed area and using 10 terms in the fitting polynomial. Figure 7 shows the improvement obtained in using 25 terms for the same data. Figures 8 and 9 are similar to Figures 5 and 6, but random background noise with an intensity of 10 per cent of the source has been added. Figure 10 shows the resolution of two 2 cm diameter sources in contact. Figure 11 shows three separated sources.

Separate programs are also available for converting the output data to iso-intensity contours or to isometric drawings that represent the activity as a third dimension, but these involve use of off-line plotting systems, and it has been elected to confine the routine output to what can be done with a fast line printer.

For kinetic studies a graphical display is used to plot the time course of the activity at a selected point. Any convenient number of such points may be selected in a given run. Figure 12 shows such a graph for the course of activity at a point in a dogs brain following injection of  $^{79}\text{Kr}$ . The first 24 points are 10 seconds apart. The last 24 points are 30 seconds apart.

#### APPLICATIONS

The original motive for constructing this instrument was for use in locating brain tumors. However it has been used in animal studies to show the time course of distribution of  $^{79}\text{Kr}$  in the brain. Similar clinical studies are scheduled to begin soon. The mechanical features of the existing system make it unsuitable for use in other areas of the body.

### FIGURE CAPTIONS

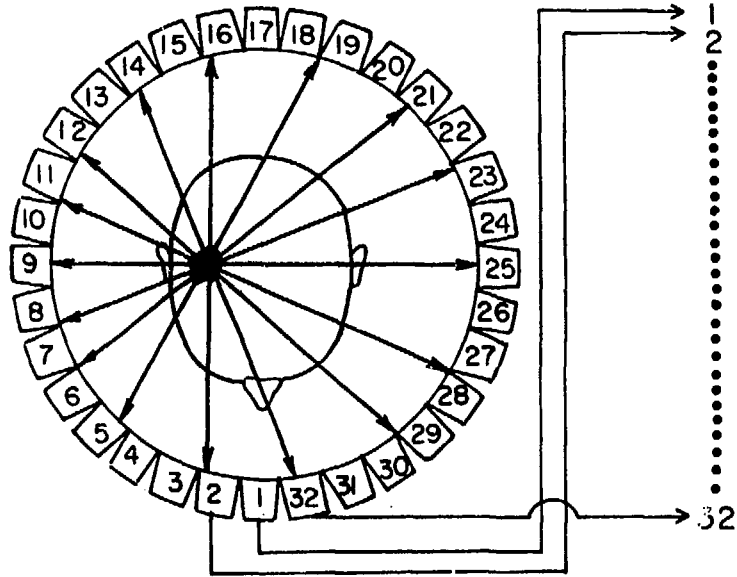
- Fig. 1 Diagram showing arrangement of 32 crystals in a ring. 0.511 MeV  $\beta^+$  annihilation gamma rays originating at the darkened spot produce coincidence counts in the counter pairs indicated by the arrows. 9-546-64
- Fig. 2 Diagram showing basis for ignoring counter pairs connected by lines that fall outside of the area of interest. 4-842-65
- Fig. 3 Photograph of apparatus showing use of a dental chair for positioning the subject. CN-10-139-62
- Fig. 4 Schematic diagram illustrating the problem involved in separating the counts due to activity in multiple sources. The analysis problem is to reconstruct the original distribution of activity from the coincidence count data. 5-579-61
- Fig. 5 Basis for the "onion peel" method of analysis. The set of counter pairs having a given separation distance is sensitive only to activity in the area further from the center than the radius of the circle defined by the connecting chords. Thus solution may proceed from the closest pairs to the most widely separated pairs with only 32 equations at each stage. 9-664-64
- Fig. 6 Digital output for a simulated source, using 10 terms in the fitting polynomial. 9-203-72
- Fig. 7 Output using the same data as in Fig. 6, but with 25 terms in the fitting polynomial. 9-198-72
- Fig. 8 Output using same data as in Fig. 6, but with random background added using 10 terms. 9-202-72

FIGURE CAPTIONS

- Fig. 9 Output for same data as Fig. 8, but using 25 terms in the analysis. 9-200-72
- Fig. 10 Resolution of two 2 cm diam sources in contact. 9-199-72
- Fig. 11 Output based on data for 3 separated sources. 9-197-72
- Fig. 12 Graph of the  $^{79}\text{Kr}$  activity at a point in a dog's brain as a function of time after injection. 9-201-72

## REFERENCES

1. F. R. Wrenn, M. L. Good and P. Handler. "The use of Positron Emitting Radioisotopes for the Localization of Brain Tumors". *Science* 113, 525-527 (1951).
2. J. L. Brownell and W. H. Sweet. "Localization of Brain Tumors with Positron Emitters". *Nucleonics* 11, No. 11, pp. 40-45 (1953).
3. G. L. Brownell, "MGH Positron Camera". Radionuclide Tomography Symposium, New York (1972).
4. S. Rankowitz, J. S. Robertson, W. A. Higinbotham and M. J. Rosenblum. "Positron Scanner for Locating Brain Tumors", 1962 IRE International Convention Record, Part 9, 49-56 (1962).
5. J. S. Robertson and A. M. Niell. "Use of a Digital Computer in the Development of a Positron Scanning Procedure". Proc. 4th IBM Medical Symposium, 77-103 (1962).
6. J. S. Robertson and S. R. Bozzo. "Positron Scanner for Brain Tumors", Proc. 6th IBM Medical Symposium, 631-645 (1964).
7. J. D. Pincus. "A Mathematical Reconstruction of a Radioactive Source Density from its Induced Radiation Pattern", BNL-AMD 539 (1964).
8. R. B. Marr. "On the Reconstruction of a Function on a Circular Domain from a Sampling of its Line Integrals", BNL-AMD 636 (1972).



$\gamma$  RAYS FROM ANNIHILATION GENERATE PULSES  
IN A 32 DETECTOR ARRAY

FIGURE 1

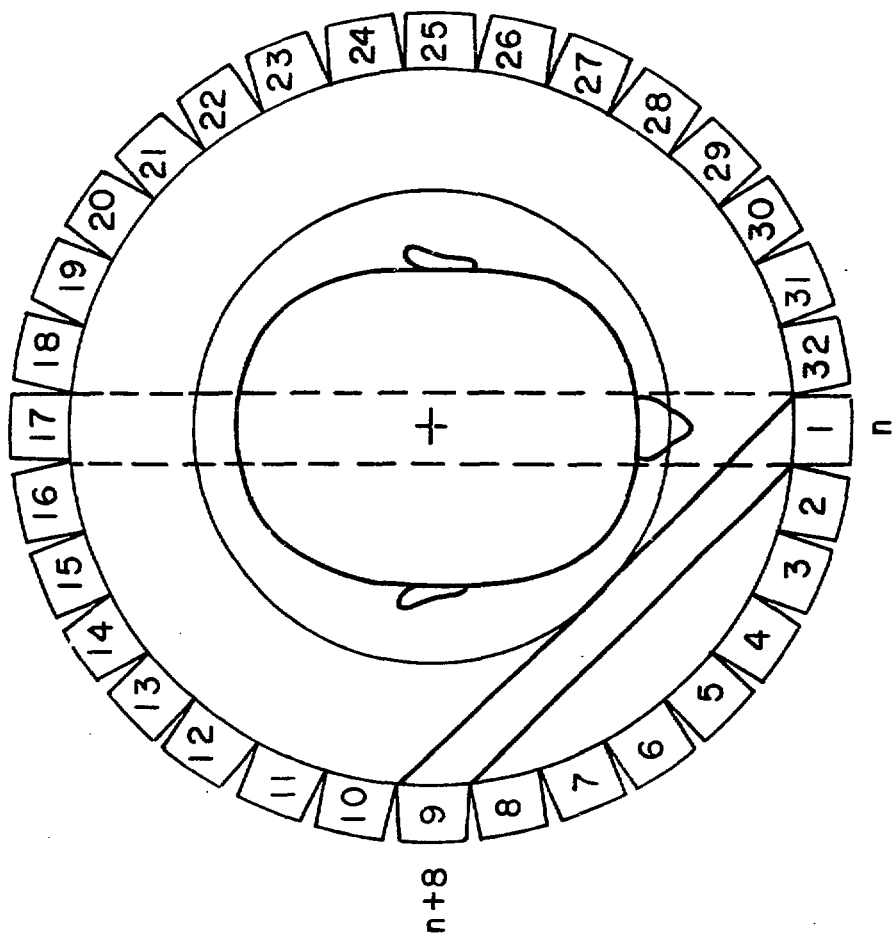


FIGURE 2

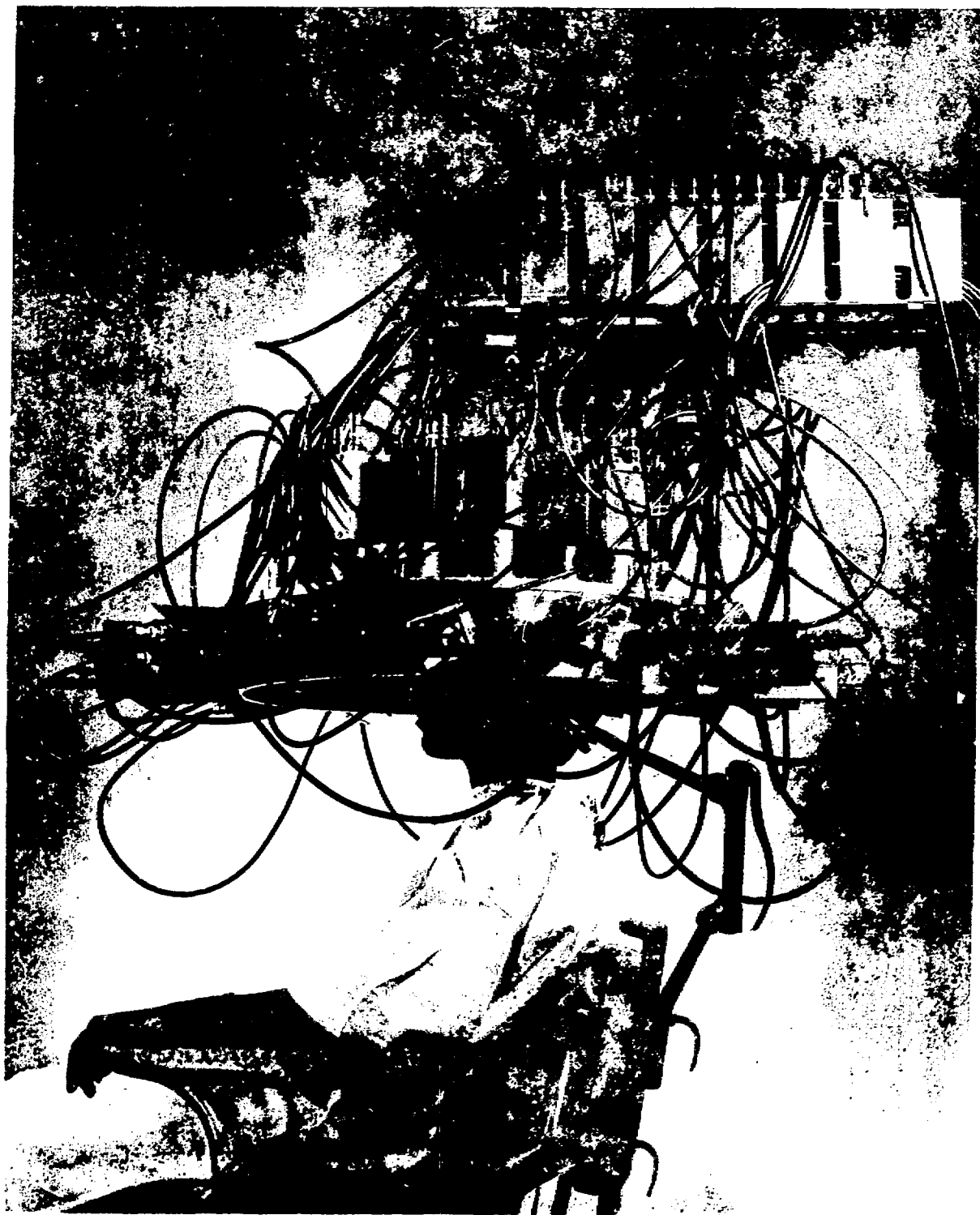
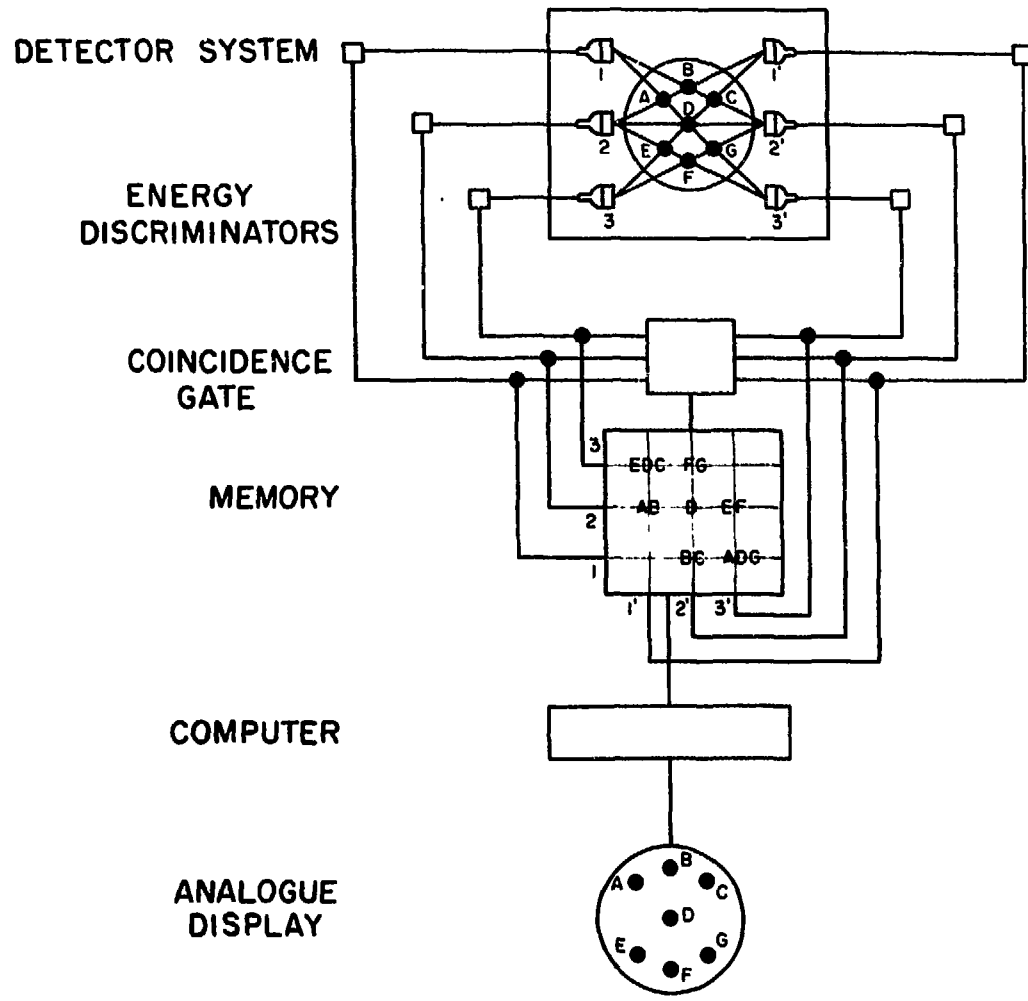
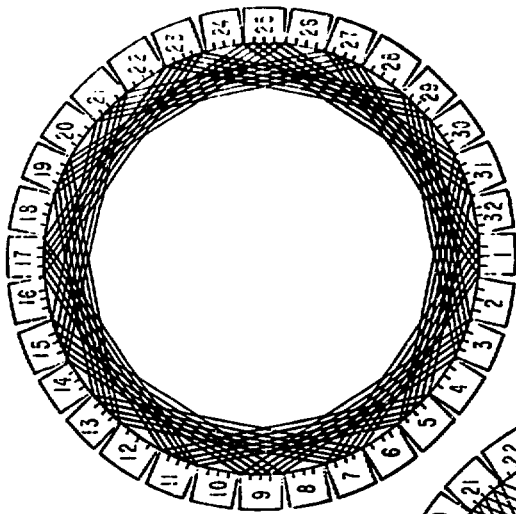


FIGURE 3

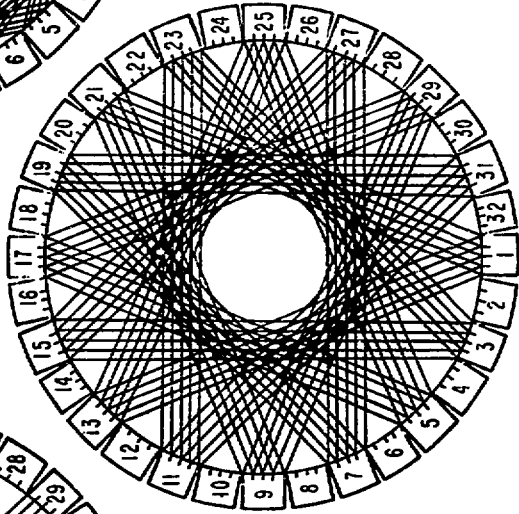


**FIGURE 4**

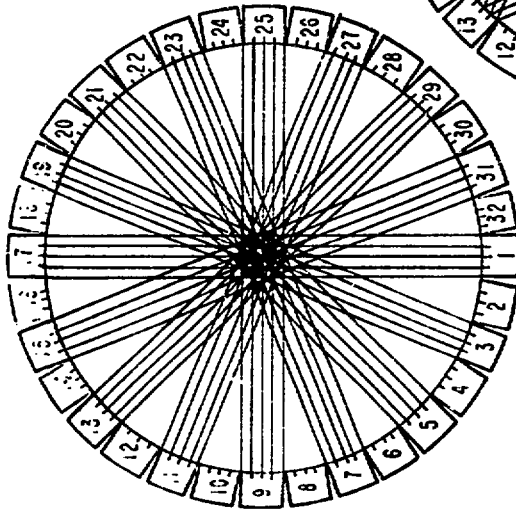




SET WITH  $N = M + 6$



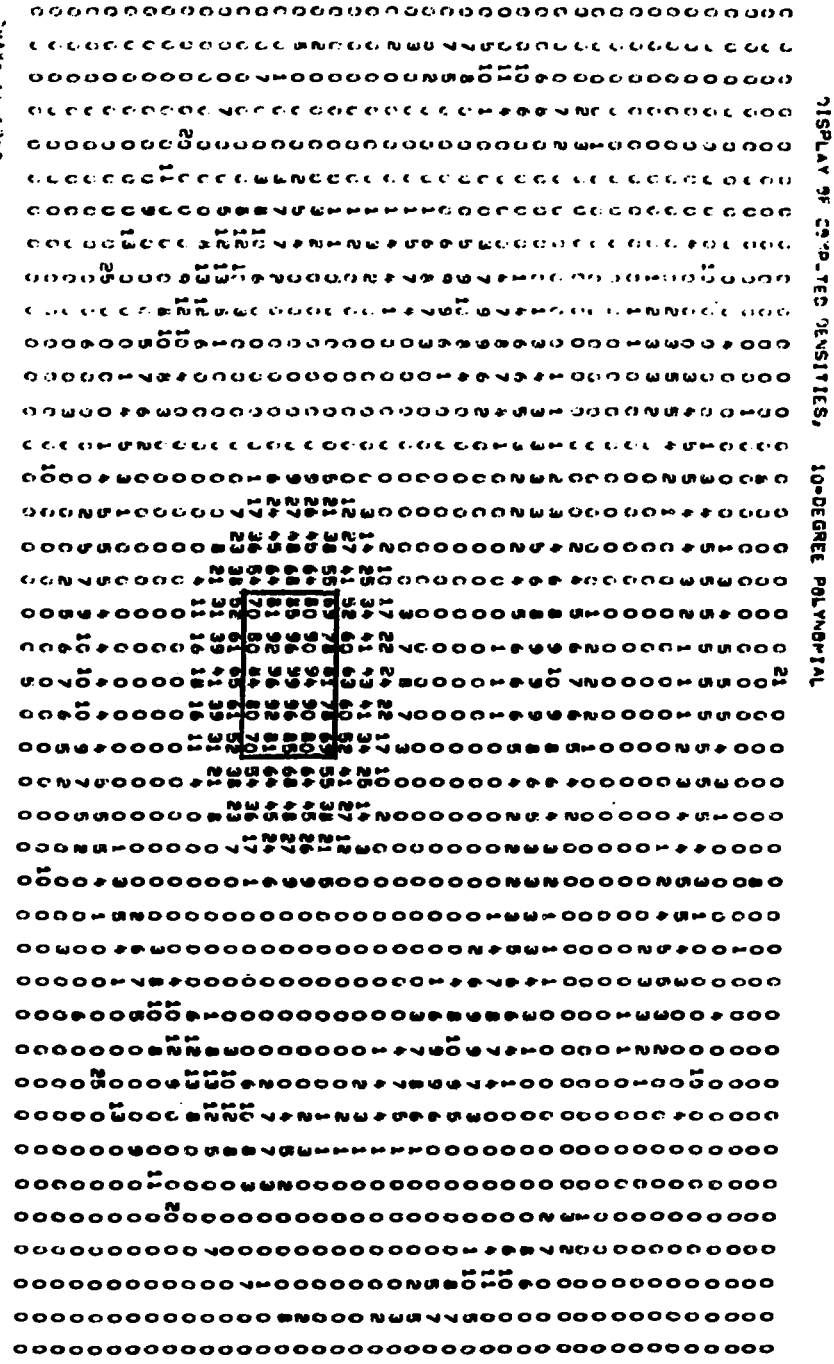
SET WITH  $N = M + 12$



SET WITH  $N = M + 16$

FIGURE 5

SIMULATED DATA FROM SEVERAL KITs ---  
 NO RANDOMIZATION  
 1000 RS = 3000 THE-TAS = 0.000000 INTENSITY= 200.0000



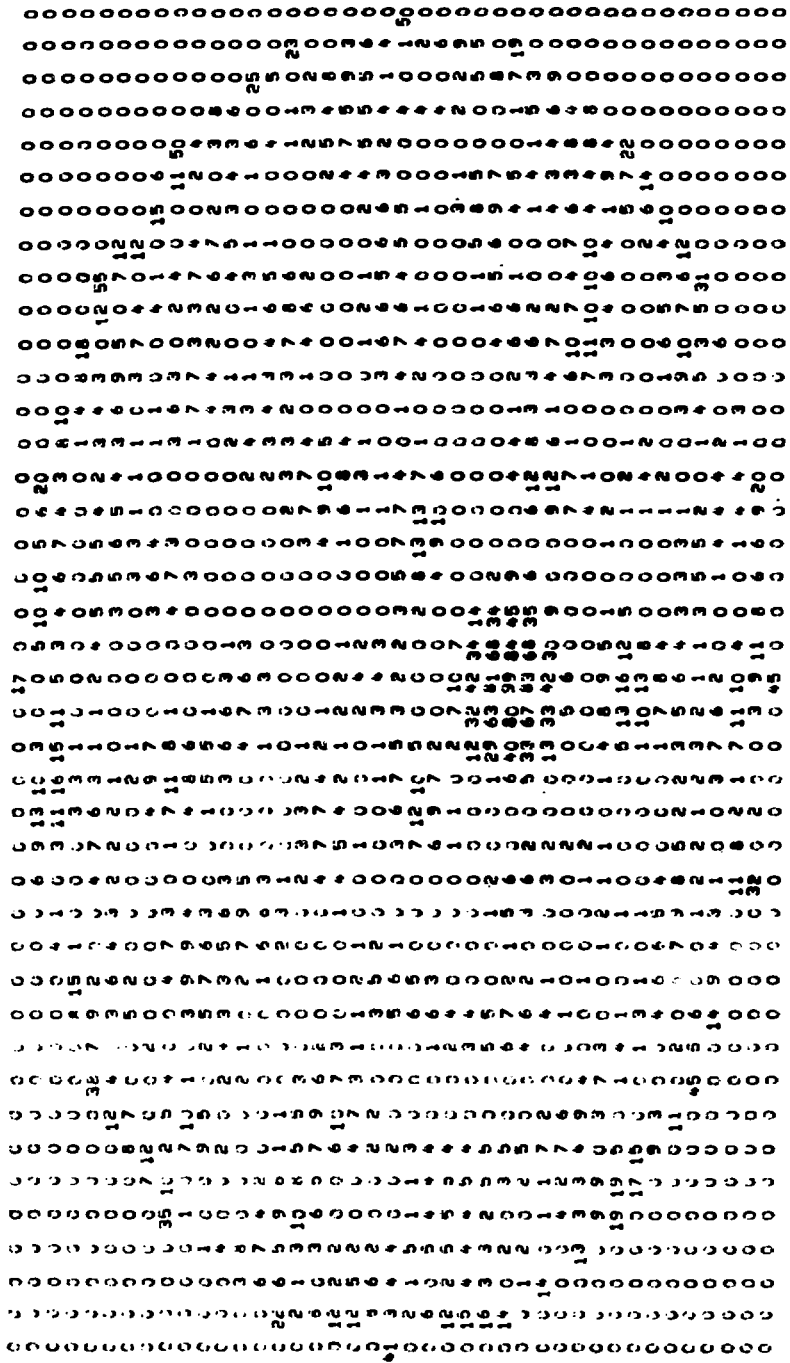
DATA 6441343

FIGURE 6





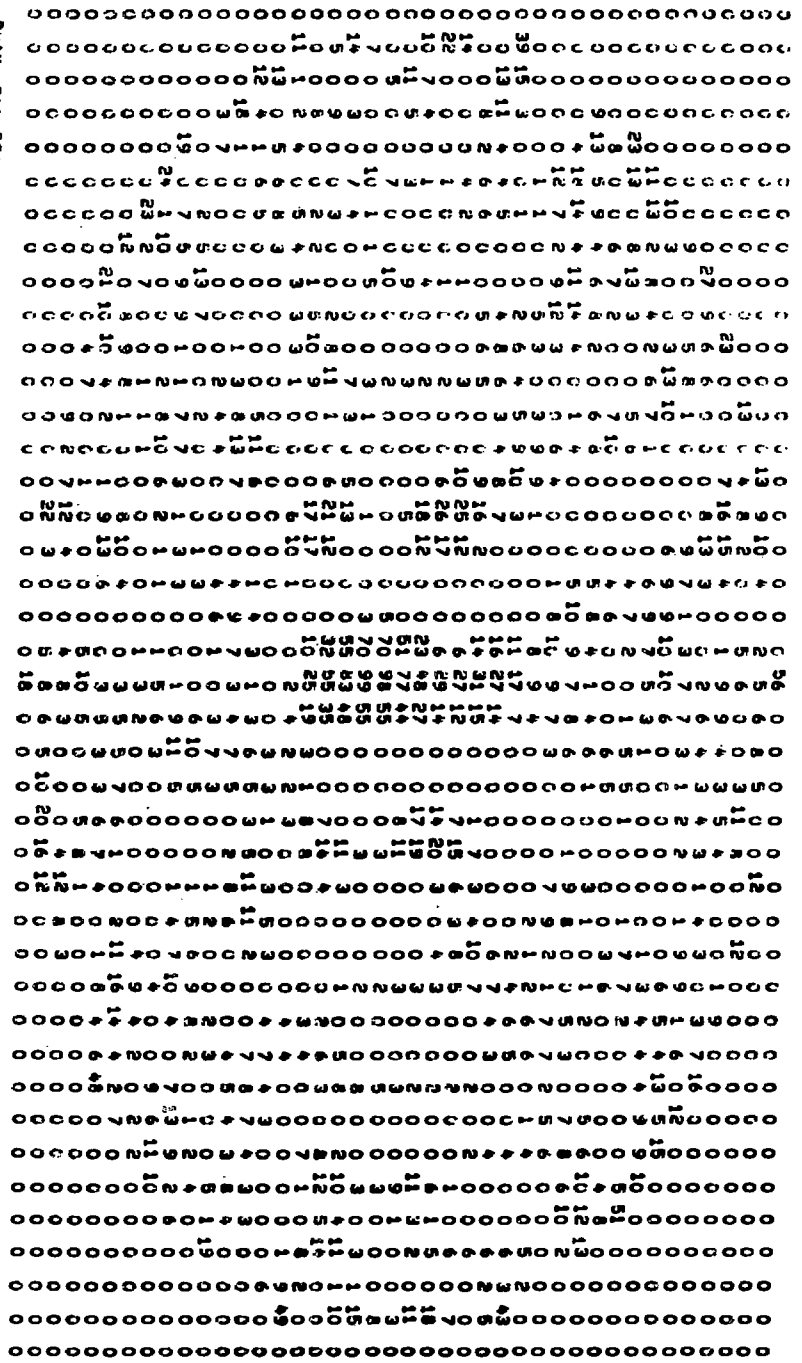
DISPLAY OF COMPUTED DENSITIES, 25-DEGREE POLYNOMIAL



DATE 2/24/66

FIGURE 9

DISPLAY OF COMPUTER DENSITIES, 30-DEGREE POLYNOMIAL



DATA 244.391

FIGURE 10

DISPLAY OF COMPUTED DENSITIES

MM#	ISX	Max(V)	15	14	13	12	11	10	9	8	7	6	5	4	3	2	1	0
0	0	0	0	1	0	0	0	0	1	2	0	0	0	0	0	0	0	0
0	0	1	1	0	0	0	0	0	1	1	0	0	0	1	2	1	0	0
0	1	2	2	1	1	0	0	1	2	1	1	1	0	0	0	1	2	2
0	1	2	2	2	2	0	0	1	0	0	0	0	0	0	2	1	0	0
0	0	1	2	3	3	1	1	1	0	0	0	0	0	0	0	0	0	0
0	0	0	1	3	2	1	1	2	2	3	3	2	0	0	0	2	6	6
0	0	0	0	1	1	0	0	1	4	5	4	1	0	0	0	0	1	6
0	0	0	0	0	1	0	0	0	3	3	3	1	0	0	0	0	0	0
0	0	0	0	1	2	1	0	0	0	1	4	6	6	3	1	0	0	2
0	1	0	0	1	2	2	0	0	0	0	3	5	2	0	0	0	0	0
1	2	0	0	0	1	3	3	0	0	0	2	1	0	0	0	0	0	0
0	0	0	0	0	0	3	4	2	0	0	4	4	0	0	0	0	0	0
0	0	0	0	0	2	5	3	0	3	3	11	7	2	1	0	7	8	7
0	0	0	0	0	0	3	2	0	2	7	4	5	2	1	2	3	5	6
0	0	0	0	0	0	0	0	0	0	0	0	0	0	0	1	0	0	0
1	0	0	0	0	0	0	0	0	0	0	0	0	0	0	0	1	27	68
2	1	0	0	0	0	0	0	0	0	0	26	60	77	61	26	0	0	0
1	1	1	3	3	1	0	0	0	0	0	6	38	80	100	80	37	0	0
0	0	2	4	5	5	3	1	1	4	2	0	0	23	57	74	58	23	0
0	0	1	2	2	4	6	5	3	4	0	0	0	15	28	19	0	0	0
0	0	1	0	0	1	6	5	1	1	4	3	0	0	0	0	0	0	0
1	0	1	0	0	0	2	1	0	0	1	3	1	0	2	0	0	0	0
1	1	0	0	0	0	0	0	0	0	0	0	0	2	12	16	9	0	0
0	1	0	0	0	0	0	0	0	0	0	0	0	0	2	25	34	20	0
0	0	0	0	0	1	0	0	0	7	6	0	0	14	54	70	51	16	0
0	0	0	0	0	2	3	0	2	7	6	0	0	35	79	100	80	39	0
0	0	0	1	0	1	4	0	3	4	1	0	0	27	64	82	66	32	0
0	1	0	1	2	1	1	1	1	0	0	0	0	5	22	31	23	7	0
0	0	1	1	1	2	1	0	0	0	0	0	0	0	1	0	0	0	0
0	0	0	1	1	0	1	1	0	0	0	1	2	1	0	0	1	0	0
0	0	0	0	1	1	0	0	0	1	1	0	0	0	0	1	1	0	0

MAX = 1289.65

FIGURE 11

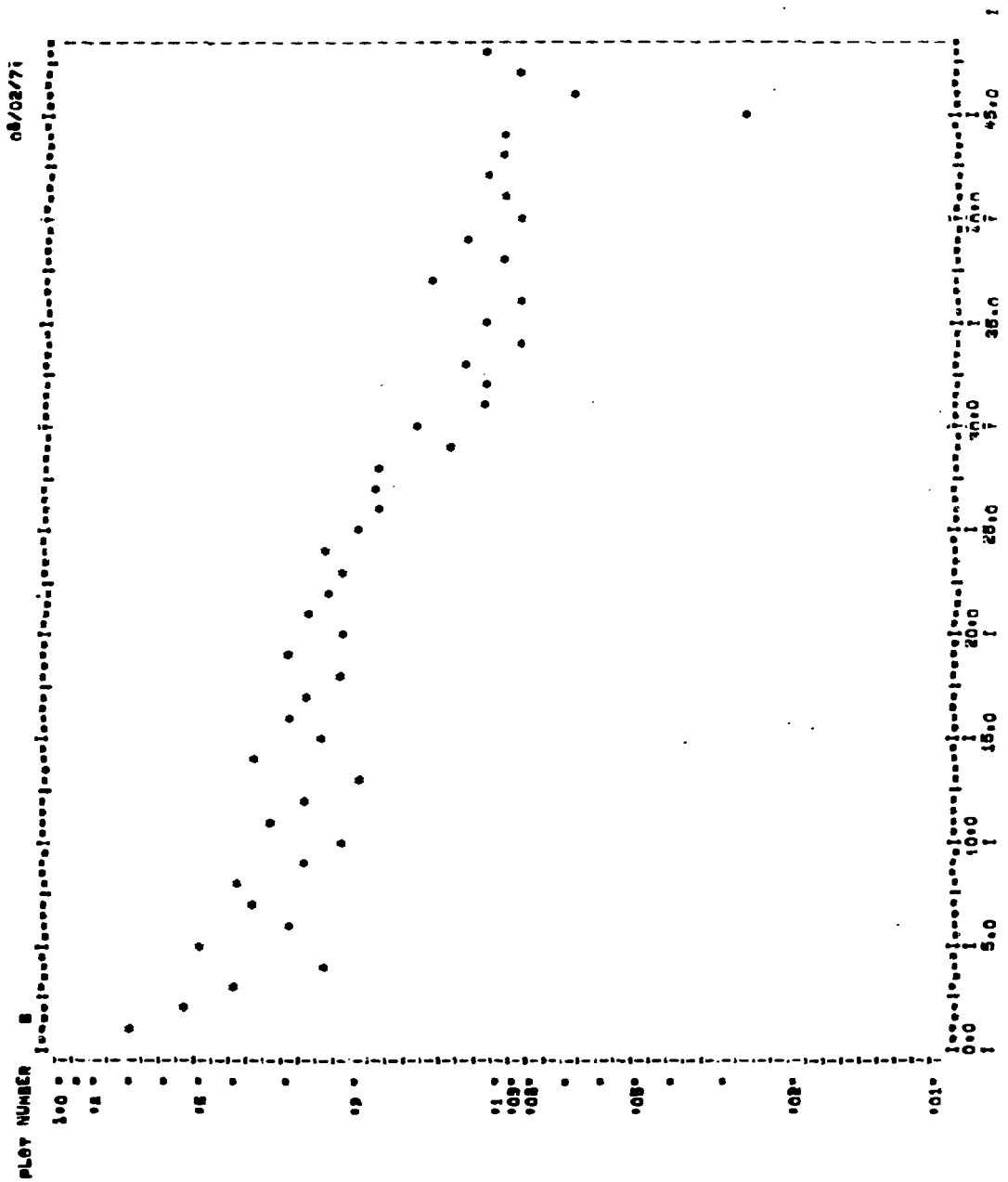


FIGURE 1 2